CORROSION SCIENCE AND TECHNOLOGY, Vol.24, No.3(2025), pp.151~161 pISSN 1598-6462 / eISSN 2288-6524
[Research Paper] DOI: https://doi.org/10.14773/cst.2025.24.3.151

Improving Insulating and Wettability Properties of Titanium Alloys via Electrochemical Anodization

Yeji Choi [1,††] and Chanyoung Jeong[1,2,†,††]

[1]*Department of Advanced Materials Engineering, Dong-eui University, Busan 47340, Republic of Korea*
[2]*The Research Institute of Advanced Functional Surface Engineering, Dong-eui University, Busan 47340, Republic of Korea*
(Received May 16, 2025; Revised June 13, 2025; Accepted June 17, 2025)

In this study, anodization was applied to Titanium (Grade 4) alloy to form nanostructured oxide films and resulting changes in surface properties were systematically investigated with respect to anodization time. As the duration of anodization increased, the oxidation reaction was intensified, leading to a progressive thickening of the TiO_2 layer. Energy Dispersive X-ray Spectroscopy (EDS) analysis confirmed a gradual increase in oxygen content with a corresponding decrease in titanium content. Additionally, enlargement of pores and surface roughness with longer anodization times resulted in reduced contact angles, indicating enhanced hydrophilicity. Electrical resistance measures revealed that thicker oxide layers effectively impeded electron flow, thereby exhibiting superior insulating characteristics than thinner oxide layers. Overall, these results demonstrate that anodization is a promising surface modification technique for a wide range of applications, including energy devices and electronic components. In particular, the TiO_2 oxide layer holds significant potential as a high-performance surface material due to its excellent insulating properties and improved wettability.

Keywords: *Titanium Anodizing, Anodizing Time, Surface Roughness, Wettability, Resistance Test*

1. Introduction

With the advancement of modern energy technologies, there has been a growing interest in next-generation energy devices such as fuel cells, water electrolysis systems, and photoelectrochemical (PEC) cells. Among their components, the performance of electrode materials —key elements in these systems—plays a critical role in determining overall device efficiency. In such applications, properties such as high electrochemical activity and surface area, excellent corrosion resistance, and long-term durability are essential requirements [1,2].

Titanium alloys are widely utilized in various fields such as biomedical engineering, aerospace, and energy industries due to their excellent mechanical strength and outstanding corrosion resistance. Titanium Grade 4, with a yield strength of approximately 480 MPa, is the strongest among commercially pure titanium grades, making it a promising candidate for structural and functional applications that demand both high strength and corrosion resistance [3,4]. Despite their favorable mechanical and chemical properties, titanium alloys face limitations in energy device applications due to their inherently low electrical conductivity and electrochemical activity [5-8]. Furthermore, when exposed to harsh or long-term operational environments, titanium alloys are susceptible to galvanic corrosion caused by potential differences when in contact with dissimilar metals, as well as the development of micro-defects, which can compromise their corrosion resistance. Therefore, surface modification is essential to enhance both durability and functionality [9-11].

To address these challenges, surface nano structuring of titanium has garnered significant attention. The formation of nanostructures such as nanotubes and nanopores increases the surface area and facilitates interfacial reactions with the electrolyte, thereby improving charge transfer and ion diffusion, which enhance electrochemical performance [12-14]. Additionally, such nanostructures help control surface wettability, contributing to more efficient gas evolution. They also enhance the adhesion of secondary processes such as coating and dyeing, while improving both electrical and electrochemical

†Corresponding author: cjeong@deu.ac.kr
††These authors contributed equally to this work as the first author. Chanyoung Jeong: Professor, Yeji Choi: Graduate Student

stability [15-18].

Various surface treatment techniques—such as sandblasting and acid etching (SLA), laser treatment, physical vapor deposition (PVD), and anodization—have been developed and employed to enhance surface functionality. While each method may be effective under specific application requirements, they often face limitations in precise nanostructure control, process reproducibility, uniformity over large areas, as well as equipment complexity and cost-efficiency [19-22]. In contrast, anodization stands out as a relatively simple and environmentally friendly electrochemical technique that enables the formation of well-defined nanostructures over large surface areas. It offers significant advantages in terms of cost-effectiveness and reproducibility [23-26]. The oxide layer formed through anodization is typically dense, hard, and highly corrosion resistant. Moreover, different nanostructures can be formed depending on various process parameters such as electrolyte type and concentration, temperature, applied current, and voltage. By adjusting these conditions, structures like nanotubes and nanopores can be selectively fabricated [27]. The key electrochemical reactions involved in the anodization of titanium are presented in equations (1) and (2), while a schematic illustration of the anodization setup is shown in Fig. 1a [28-31].

$$Ti + 2H_2O \rightarrow TiO_2 + 4\,H^+ \quad (1)$$

$$TiO_2 + 6F^- \rightarrow [TiF_6]^{2-} + 2H_2O + 2H^+ \quad (2)$$

During anodizing process, the loss of electrons leads to the formation of an oxide layer through the combination of titanium ions with hydroxide ions and oxygen. In electrolytes containing fluoride ions (F^-), the oxide layer undergoes selective dissolution, resulting in the self-organized growth of nanoporous structures. The formation process of these self-aligned TiO_2 pores is illustrated in Fig. 1b [32-34]. This simultaneous chemical dissolution influences pore diameter, spacing, and morphology, allowing for the fabrication of tailored nanostructures through precise control of process parameters. Such nanostructures offer enhanced surface activity, high photo-responsiveness, and excellent electrochemical stability, making them highly promising for application in a wide range of energy conversion and storage devices, including fuel cells and water-splitting systems [35-38].

In this study, anodization was applied to Titanium Grade 4 alloy to fabricate nanostructured oxide films. The effects of anodization on surface roughness, wettability, and the relationship between oxide layer thickness and electrical resistance were systematically investigated. Surface characteristics were compared with respect to varying

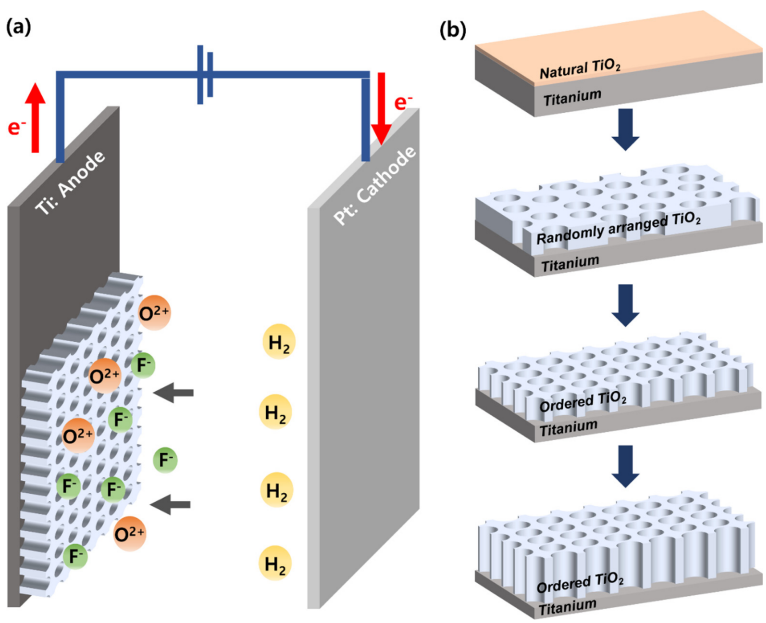

Fig. 1. (a) Titanium anodizing mechanism schematic (b) TiO_2 film formation process

anodization durations, and the feasibility of surface modification for energy-related applications was evaluated.

2. Experimental Methods

2.1 Experimental method

For this study, Titanium Grade 4 alloy sheets were cut into specimens measuring 2.5 × 3 cm, providing a surface area of 7.5 cm^2. To remove organic contaminants and surface impurities, the specimens underwent ultrasonic cleaning in acetone, ethanol, and deionized water, sequentially, followed by drying. The cleaned samples were then subjected to electropolishing to eliminate the native oxide layer and to achieve surface leveling. This was performed in an electrolyte composed of perchloric acid (70%) and acetic acid mixed in a 1:5 volume ratio. Electropolishing was conducted under a constant voltage of 35 V for 10 minutes using a DC power supply. Subsequently, to fabricate nanostructured oxide layers on the titanium surface, anodization was carried out in an electrolyte consisting of 14.5 M ethylene glycol ($C_2H_6O_2$), 1 M distilled water (H_2O), and 0.07 M ammonium fluoride (NH_4F). A constant voltage of 40 V was applied for a duration ranging from 1 to 6 hours.

2.2 Nanostructures analysis

To precisely observe and analyze the microstructure and pore characteristics of the oxide layer formed after anodization, a high-resolution field emission scanning electron microscope at the Converging Materials Core Facility of Dong-eui University (FE-SEM) was employed. This allowed for visual assessment of the surface morphology, structural features of the pores, pore distribution, and overall structural uniformity of the oxide layer. Quantitative analysis of the high-resolution images was conducted using ImageJ software, which enabled measurement of average pore diameter, inter-pore distance, oxide layer thickness. Then, atomic force microscope at the Converging Materials Core Facility of Dong-eui University (AFM, NITECH, SPA-400) was used to observe the roughness of the oxide film according to anodizing time.

Elemental composition and spatial distribution of the oxide layer were investigated using energy-dispersive spectroscopy at the Converging Materials Core Facility of Dong-eui University (EDS), integrated with the FE-SEM system. EDS provided both qualitative identification and quantitative analysis of the elemental constituents present on the specimen surface.

Surface wettability was assessed using a contact angle meter (Smart Drop, Femtobiomed Inc.). A 3 μL droplet of distilled water was statically applied to each sample, and contact angles were measured under identical conditions. For each specimen, ten measurements were taken and averaged, with standard deviations calculated to ensure reproducibility.

To evaluate the influence of oxide layer thickness on electrical properties, resistance testing was performed. Measurements were repeated ten times under consistent conditions for each sample, and average values and error ranges were calculated. This enabled a systematic comparison of the changes in electrical resistance and insulation behavior associated with oxide layer growth.

Subsequently, to evaluate corrosion resistance, electrochemical polarization tests were carried out using a three-electrode cell in a 3.5 wt% NaCl solution. An Ag/AgCl electrode was employed as the reference electrode, and a platinum mesh served as the counter electrode. Titanium specimens anodized for varying durations were used as the working electrodes. Prior to the potentiodynamic polarization (PDP) test, the open circuit potential (OCP) was monitored for 1 hour to ensure stabilization of the potential.

3. Results

3.1 Morphological and structural analysis of anodized titanium

Fig. 2 presents FE-SEM images of the TiO_2 surface obtained at various anodization durations, showing top, tilted, and cross-sectional views. Quantitative values derived from these observations—namely, pore diameter, inter-pore distance, and oxide layer thickness—are summarized in Table 1. This data is further visualized as graphs in Figs. 3 and 4. Analysis of the top and tilted views revealed that as the anodization time increased, the average pore diameter grew from 38.11 ± 6.36 nm to 52.55 ± 5.03 nm, while the inter-pore distance expanded from 72.74 ± 4.11 nm to 93.21 ± 6.27 nm. As shown in Fig. 3, these changes exhibited a linear trend with respect

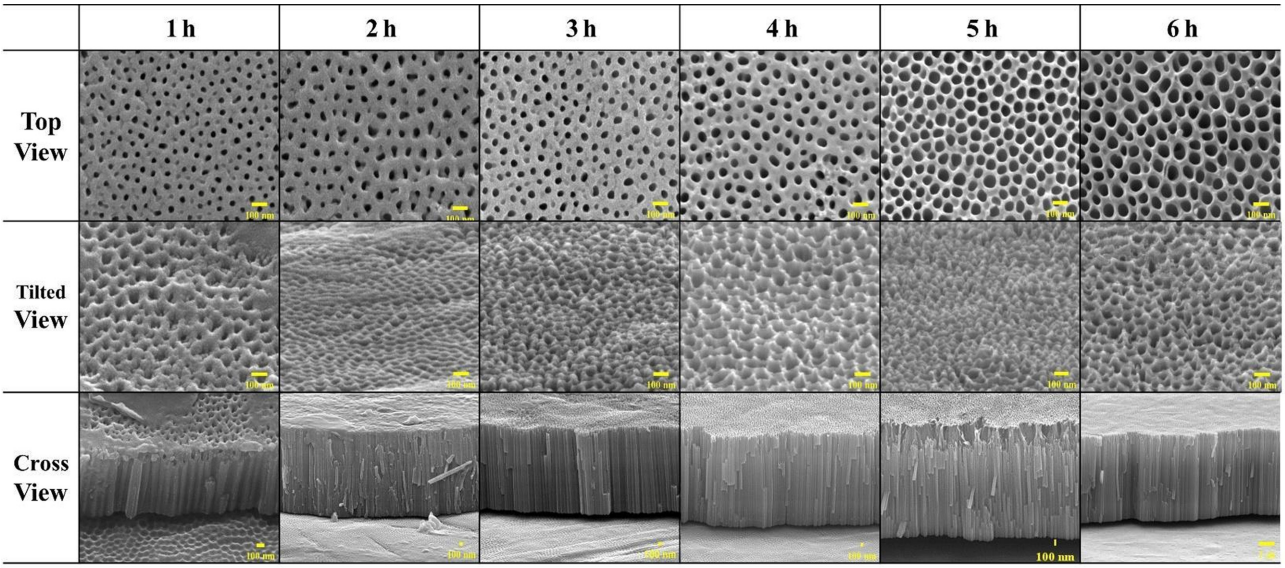

Fig. 2. FE-SEM image of TiO_2 morphology as a function of anodizing time

Table 1. Surface morphology parameters of oxide film according to anodizing time

Time (h) Parameters	1 h	2 h	3 h	4 h	5 h	6 h
Pore diameter (nm)	38.11 ± 6.36	39.71 ± 5.38	41.70 ± 5.36	43.79 ± 4.82	50.99 ± 4.18	52.55 ± 5.03
Interpore distance (nm)	72.74 ± 4.11	77.31 ± 6.61	82.86 ± 7.50	83.79 ± 2.28	88.03 ± 8.27	93.21 ± 6.27
Thickness (㎛)	0.73 ± 0.002	2.30 ± 0.02	2.34 ± 0.04	3.46 ± 0.04	4.18 ± 0.069	4.73 ± 0.05

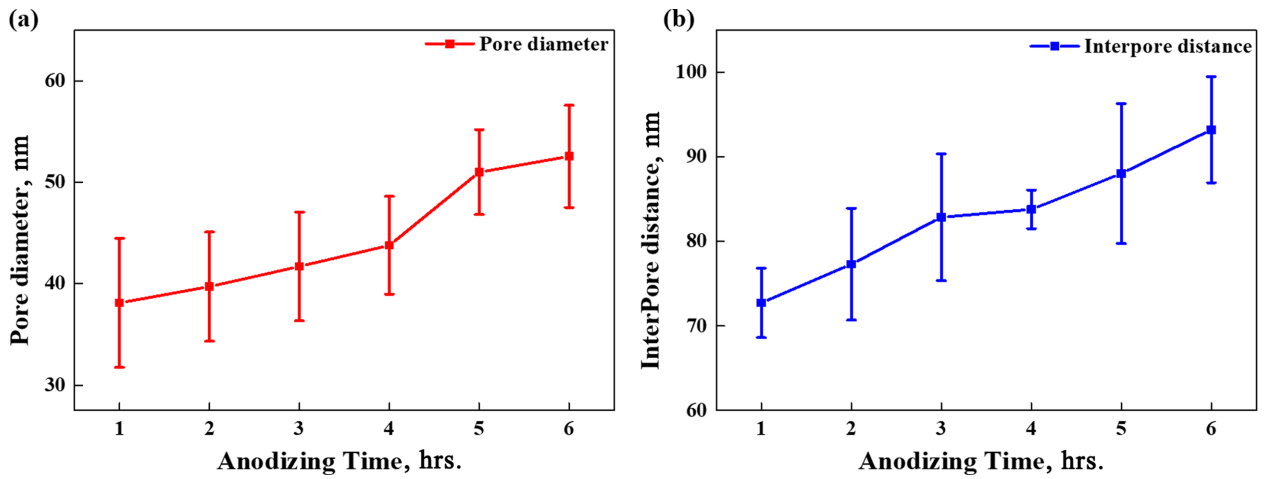

Fig. 3. Morphological parameters of TiO_2: (a) Pore diameter, (b) Interpore distance

to processing time. Cross-sectional analysis further demonstrated that the oxide film thickness increased significantly, from 0.73 ± 0.002 μm initially to 4.73 ± 0.05 μm after extended anodization, showing an approximately 6.47 times increase in thickness. These results indicate that longer anodization durations lead to increased ionic activity at the metal surface, promoting the growth of a porous oxide layer. Consequently, structural evolution is observed in the form of enlarged pore diameters, increased spacing, and thicker oxide films.

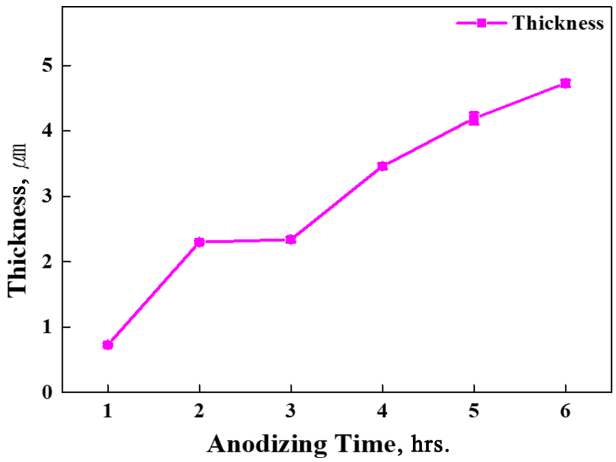

Fig. 4. Variation in titanium oxide film thickness according to anodizing time

3.2 Surface composition analysis

Fig. 5 and Table 2 present the quantitative analysis of titanium and oxygen content as a function of anodization time, as measured by energy-dispersive X-ray spectroscopy (EDS). Prior to anodization, the titanium and oxygen contents were measured at 94.82 wt% and 5.18 wt%, respectively. As the anodization duration increased, the titanium content decreased progressively to 76.16 wt%, 69.64 wt%, 65.73 wt%, 60.81 wt%, 57.45 wt%, and 52.33 wt%, while the oxygen content correspondingly increased to 23.84 wt%, 30.36 wt%, 34.27 wt%, 39.19 wt%, 42.55 wt%, and 47.67 wt%. These trends indicate that during the anodization process, titanium undergoes oxidation, forming a TiO_2 based oxide layer. The continuous increase in oxygen content, along with the gradual depletion of titanium, serves as an indirect indicator of oxide layer growth and thickness evolution. This progression suggests that the anodic oxidation reaction proceeds steadily over time, contributing to the formation of a denser and thicker oxide film.

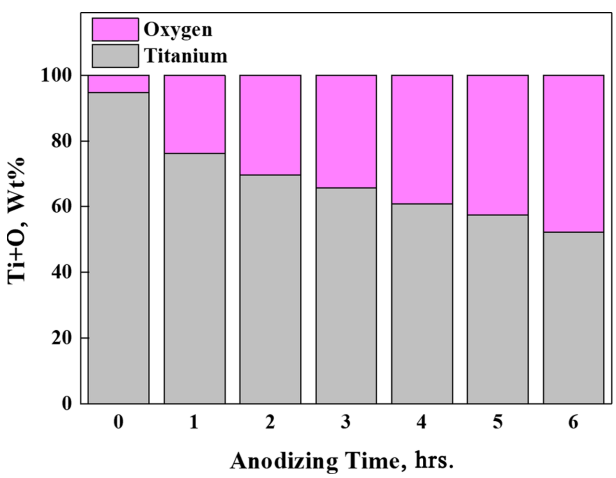

Fig. 5. Qualitative and quantitative analysis of Ti and O elemental composition according to anodizing time

3.3 Evaluation of TiO_2 surface properties

Fig. 6 displays atomic force microscopy (AFM) images illustrating the surface roughness of the oxide layers formed after various anodization durations. For each sample, the average surface roughness (R_a) was measured three times from the reference plane to the designated surface, and the corresponding mean values and standard

Table 2. Titanium and oxygen contents of TiO_2 film analyzed by Energy Dispersive Spectroscopy

Wt% Time (h)	Ti	O
0	94.82	5.18
1	76.16	23.84
2	69.64	30.36
3	65.73	34.27
4	60.81	39.19
5	57.45	42.55
6	52.33	47.67

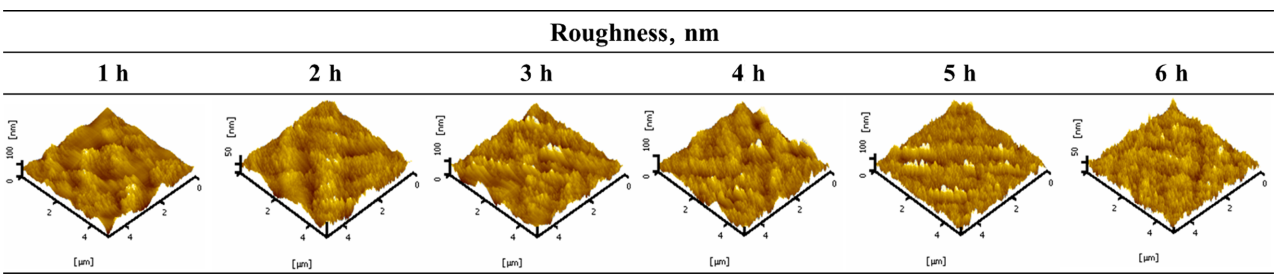

Fig. 6. Surface roughness of anodized titanium surfaces using AFM analysis

Table 3. Comparison of surface roughness of titanium alloys according to anodizing time

Time (h) Parameter	1 h	2 h	3 h	4 h	5 h	6 h
Roughness (nm)	6.75 ± 2.44	7.75 ± 1.81	8.97 ± 0.65	9.07 ± 1.31	9.98 ± 1.49	12.40 ± 2.18

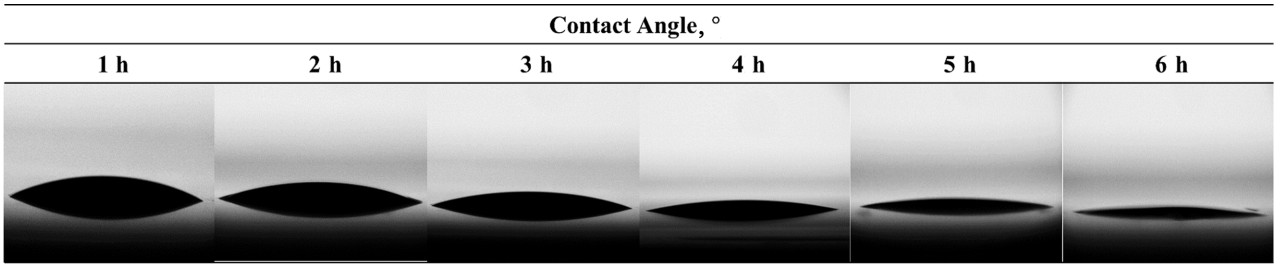

Fig. 7. Wettability evaluation of TiO_2 by contact angle measurements

Table 4. Effect of anodizing time on TiO_2 wettability values

Time (h) Parameter	1 h	2 h	3 h	4 h	5 h	6 h
Contact Angle (°)	34.43 ± 3.80	28.53 ± 1.86	22.73 ± 6.45	19.77 ± 1.30	12.63 ± 1.33	6.56 ± 4.11

deviations are summarized in Table 3. The surface roughness values for the oxide films were found to be 6.75 ± 2.44 nm, 7.75 ± 1.81 nm, 8.97 ± 0.65 nm, 9.07 ± 1.31 nm, 9.98 ± 1.49 nm, and 12.40 ± 2.18 nm, with the highest roughness observed after 6 hours of anodization. This trend suggests that as the anodization time increases, the oxide layer not only grows but also undergoes partial dissolution. This selective dissolution is more pronounced at the edges or peaks of relatively thin-walled pores, resulting in a rougher and more heterogeneous surface morphology [40].

Fig. 7 displays contact angle images representing the surface wettability of the oxide layers formed after anodization, and the corresponding average values with standard deviations are summarized in Table 4. The measured contact angles were 34.43 ± 3.80°, 28.53 ± 1.86°, 22.73 ± 6.45°, 19.77 ± 1.30°, 12.63 ± 1.33°, and 6.56 ± 4.11°, respectively. As the anodization time increased, the formation of a thicker oxide layer on the titanium surface was observed, accompanied by a noticeable enlargement in pore size. These porous structures contribute to an increase in the surface's average roughness (R_a), which in turn enhances the solid–liquid interfacial area, thereby influencing surface wettability. Wettability is typically evaluated using static contact angle measurements, and the relationship between contact angle and surface roughness can be interpreted through Wenzel's theory. According to Wenzel, the apparent contact angle (θ*) on a rough surface is related to the intrinsic contact angle (θ) on an ideal flat surface through equation (1), which accounts for the actual roughness [39].

$$\cos\theta^* = r \cdot \cos\theta \quad (1)$$

In this context, r represents the surface roughness factor. For hydrophilic surfaces, an increase in r leads to an increase in the value of cos θ*, thereby resulting in a lower apparent contact angle (θ*) and enhanced wettability. As shown in Fig. 7, longer anodization durations promoted the growth of porous structures and increased surface roughness, which in turn contributed to a progressive enhancement of surface hydrophilicity.

To evaluate the effect of oxide layer thickness on electrical resistance, resistance measurements were performed, with the quantitative results summarized in Table 5 and visualized in Fig. 8. As the anodization time increased, the electrical resistance was measured to be 20.37 ± 6.45 MΩ, 36.60 ± 4.04 MΩ, 51.62 ± 1.39 MΩ, 68.50 ± 1.39 MΩ, 93.65 ± 6.58 MΩ, and 101.43 ± 3.79 MΩ, respectively. These results reflect a significant increase in resistance corresponding to longer anodization

Table 5. Influence of TiO_2 thickness on electrical resistance values

Time (h) Parameter	1 h	2 h	3 h	4 h	5 h	6 h
Resistance Value (MΩ)	20.37 ± 6.45	36.30 ± 4.04	51.62 ± 1.39	68.50 ± 5.07	93.65 ± 6.58	101.43 ± 3.79

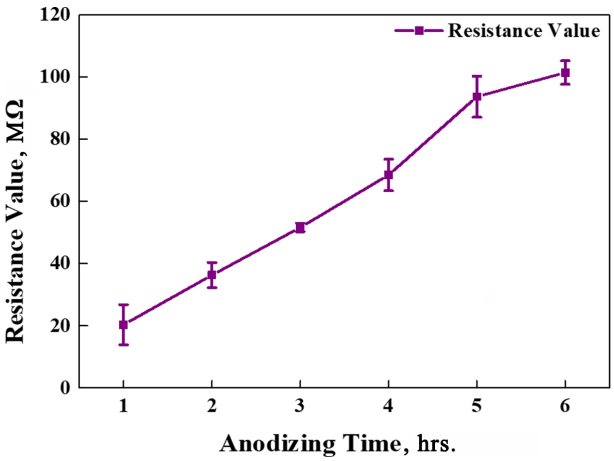

Fig. 8. Electrical resistance analysis of TiO_2 surface

times. This trend is attributed to the formation of TiO_2 on the titanium surface—an intrinsically insulating oxide—which fundamentally alters the material's electrical properties. When the oxide layer is thin, partial electron conduction may still occur either through the oxide or via pore channels. However, as the film thickens, these pathways are physically blocked, leading to a substantial rise in resistance [40]. This phenomenon is also associated with reduced capacitance and increased impedance. From an electrical perspective, the oxide film can be modeled as a metal–insulator–metal (MIM) structure, in which the resistance (R) varies as a function of the oxide thickness (d), following equation (2).

$$R = \rho \cdot \frac{d}{A} \tag{2}$$

In equation (2), ρ represents the intrinsic resistivity of the oxide film, d denotes the film thickness, and A is the effective cross-sectional area. As indicated by the equation, resistance increases linearly with thickness, and this effect becomes more pronounced when ρ is high, as in the case of insulating materials. Fig. 8 and Table 5 clearly demonstrate that the overall electrical resistance of the specimen increases with greater oxide thickness. This suggests that not only is the current flow physically impeded by the thickened oxide layer, but also that the insulating barrier formed by the anodic film is more effective at blocking electron transport than the limited conduction pathways available through pores. These observations support the interpretation that oxide thickness is a critical factor influencing the electrical insulation performance of anodized titanium [41-43].

Fig. 9 presents the potentio-dynamic polarization curves of titanium surfaces subjected to anodization for varying durations. The electrochemical parameters derived from these measurements are summarized in Table 6.

All anodized specimens exhibited a positive shift in corrosion potential (E_{corr}) compared to bare titanium, suggesting enhanced corrosion resistance due to the formation of protective oxide layers. Furthermore, the corrosion current density (I_{corr}) decreased progressively with increasing anodization time, with the specimen treated for 6 hours demonstrating the lowest I_{corr} indicative of the most effective corrosion protection. The anodized samples also showed evidence of passivation behavior, characterized by the formation of a stable oxide film that acts as a barrier to further corrosion. Notably, the

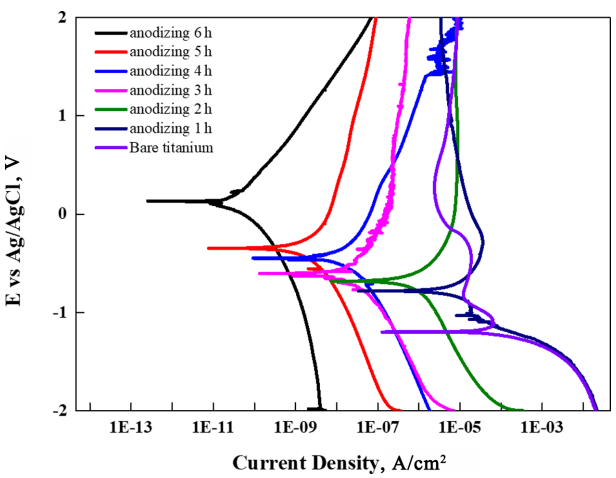

Fig. 9. Potentio-dynamic polarization analysis of TiO_2 surface

Table 6. Electrochemical corrosion parameters of anodized TiO_2 surfaces

Time (h) Parameters	0 h	1 h	2 h	3 h	4 h	5 h	6 h
β_a	0.23	0.13	0.12	0.16	0.08	0.04	0.04
β_c	0.12	0.13	0.13	0.05	0.12	0.05	0.04
Rp	8.81×10^9	6.65×10^7	7.90×10^6	3.80×10^6	1.40×10^5	1.06×10^4	7.02×10^2
I_{corr} (A/cm^2)	2.52×10^{-12}	1.44×10^{-10}	3.61×10^{-8}	4.32×10^{-9}	1.86×10^{-7}	3.16×10^{-6}	1.36×10^{-5}
E_{corr} (V)	0.09	-0.34	-0.43	-0.63	-0.68	-0.79	-1.19

specimens anodized for 5 and 6 hours displayed wide and stable passive regions, implying the formation of thick, compact, and uniform oxide layers. In contrast, samples treated for only 1 to 2 hours exhibited narrower and less stable passivation behavior, suggesting thinner and less protective oxide films. These findings confirm that the duration of the anodization process plays a critical role in determining the electrochemical stability and protective quality of the TiO_2 layer. Extended anodization times significantly improve corrosion resistance by promoting the growth of dense and homogeneous oxide coatings.

4. Conclusions

In this study, nanostructured oxide layers were fabricated on Titanium Grade 4 alloy via anodization, with processing time used as the main variable. The influence of anodization duration on surface roughness, wettability, and electrical resistance was systematically investigated. As the anodization time increased, the number of reactive ions at the metal–electrolyte interface grew, promoting the structural growth of the oxide layer. EDS analysis confirmed a gradual increase in oxygen content and a corresponding decrease in titanium content over time, indicating the progressive formation of a TiO_2 oxide layer through oxidation reactions.

Furthermore, extended anodization resulted in localized dissolution on the surface, leading to enlarged pore diameters and increased surface roughness. These porous structures were found to enhance surface hydrophilicity, as demonstrated by contact angle measurements. Electrical resistance analysis showed that the thickened oxide layer effectively blocked electron pathways, thus improving insulation performance.

Based on these findings, anodization emerges as a promising technique for the surface modification of titanium in various industrial applications, including biomedical materials, energy devices, and electronic components. The excellent biocompatibility, insulating properties, increased surface roughness, and enhanced wettability of the TiO_2 oxide layer make it a strong candidate for applications such as medical implants, battery electrodes, and sensor devices. As such, anodization holds significant potential as a surface engineering technology for fabricating high-performance functional oxide films.

Acknowledgment

This work was supported by Dong-eui University Foundation Grant (2024).

References

1. I. P. T. Avila, R. M. Souza, A. C. Ulloa, P. A. R. Trabolsi, R. T. Rosas, R. C. Espinoza, E. H. Sanchez, Effect of Anodization Time on the Adhesion Strength of Titanium Nanotubes Obtained on the Surface of the Ti-3Al-4V Alloy by Anodic Oxidation, *crystal*, **13**, 1059 (2023). Doi: https://doi.org/10.3390/cryst13071059
2. S. Durdu, G. Cihan, E. Talcin, A. Altinkok, Characterization and Mechanical Properties of TiO_2 Nanotubes Formed on Titanium by Anodic Oxidation, *Ceramics International*, **47**, 10972 (2021). Doi: https://doi.org/10.1016/j.ceramint.2020.12.218
3. Y. Choi, C. Jeong, Influence of Electrolyte on the Shape and Characteristics of TiO_2 during Anodic Oxidation of Titanium, *Corrosion Science and Technology*, **22**, 193 (2023). Doi: https://doi.org/10.14773/cst.2023.22.3.193
4. T. Dikici, M. Toparli, Microstructure and Mechanical Properties of Nanostructures and Microstructured TiO_2

Films, *Materials Science & Engineering A*, **661**, 19 (2016). Doi: https://doi.org/10.1016/j.msea.2016.03.023
5. S. H. Kim. C. Jeong, Feasibility of Machine Learning Algorithms for Predicting the Deformation of Anodic Titanium Films by Modulating Anodization Processes, *Materials*, **14**, 1089 (2021). Doi: https://doi.org/10.3390/ma14051089
6. J. Kim, C. Jeong, Investigation of Functional 6061 Aluminum Alloy Oxide Film with Anodization Voltage and Its Corrosion Resistance, *Corrosion Science and Technology*, **22**, 399 (2023). Doi: https://doi.org/10.14773/cst.2023.22.6.399
7. J. Kim, C. Jeong, A Study on the Surface Properties and Corrosion Behavior of Functional Aluminum 3003 Alloy using Anodization Method, *Corrosion Science and Technology*, **21**, 290 (2022). Doi: https://doi.org/10.14773/cst.2022.21.4.290
8. J. M. Jáquez-Muñoz, C. Gaona-Tiburcio, C. T. Méndez-Ramírez, M. Á. Baltazar-Zamora, F. Estupinán-López, R. G. Bautista-Margulis, and F Almeraya-Calderón, Corrosion of Titanium Alloys Anodized Using Electrochemical Techniques, *Metals*, **13**, 476 (2023). Doi: https://doi.org/10.3390/met13030476
9. A. K. Sharma, Anodizing Titanium for Space Applications, *Thin Solid Films*, **208**, 48 (1992). Doi: https://doi.org/10.1016/0040-6090(92)90946-9
10. P. Shi, F. T. Cheng, H. C. Man, Improvement in Corrosion Resistance of NiTi by Anodization in Acetic Acid, *Materials Letters*, **61**, 2385 (2007). Doi: https://doi.org/10.1016/j.matlet.2006.09.020
11. H. Ji, C. Jeong, Study on Corrosion and Oxide Growth Behavior of Anodized Aluminum 5052 Alloy, *Journal of Surface Science and Engineering*, **51**, 372 (2018). Doi: https://doi.org/10.5695/JKISE.2018.51.6.372
12. C, Jeong, A Study on Functional Hydrophobic Stainless Steel 316L Using Single-Step Anodization and a Self-Assembled Monolayer Coating to Improve Corrosion Resistance, *Coatings*, **12**, 395 (2022). Doi: https://doi.org/10.3390/coatings12030395
13. J. Lu, J. Zhang, P. Hou, Y. Liu, Z. Li, P. Lu, G. Wen, L. Liu, H. Sun, Preparation, Optical Properties, and Color Formation Mechanism of Tantalum Oxide Anode Films, *Optical Materials*, **136**, 113425 (2023). Doi: https://doi.org/10.1016/j.optmat.2022.113425
14. C. Jeong, C. H. Choi, Single-step Direct Fabrication of Pillar-on-pore Hybrid Nanostructures in Anodizing Aluminum for Superior Superhydrophobic Efficiency, *ACS Applied Materials & Interfaces*, **4**, 842 (2012). Doi: https://doi.org/10.1021/am201514n
15. C. Jeong, J. Lee, K. Sheppard, C. H. Choi, Air-impregnated Nanoporous Anodic Aluminum Oxide Layers for Enhancing the Corrosion Resistance of Aluminum, *Langmuir*, **31**, 11040 (2015). Doi: https://doi.org/10.1021/acs.langmuir.5b02392
16. C. Jeong, Nano-engineering of Superhydrophobic Aluminum Surface for Anti-corrosion, Stevens Institute of Technology, Hoboken, NJ, 2 (2013). https://ui.adsabs.harvard.edu/abs/2013PhDT.....45J/abstract
17. S. L. de Assis, S. Wolynec, I. Costa, Corrosion Characterization of Titanium Alloys by Electrochemical Techniques, *Electrochimica Acta*, **51**, 1815 (2006). Doi: https://doi.org/10.1016/j.electacta.2005.02.121
18. S. Berger, J. Kunze, P. Schmuki, D. Leclere, A.T. Valota, P. Skeldon, G. E. Thompson, A Lithographic Approach to Determine Volume Expansion Factors During Anodization: Using the Example of Initiation and Growth of TiO_2 Nanotubes, *Electrochimica Acta,* **57**, 5942 (2009). Doi: https://doi.org/10.1016/j.electacta.2009.05.064
19. A. Z. Sadek, H. Zheng, K. Latham, W. Wlodarski, K. Kalantar-zadeh, Anodization of Ti thin film deposited on ITO, *Langmuir,* **25**, 509 (2009). Doi: https://doi.org/10.1021/la802456r
20. K. Kim, B.A. Lee, X.H. Piao, H.J. Chung, Y.J. Kim, Surface Characteristics and Bioactivity of Anodized Titanium Surface, *Journal of Periodontal & Implant Science*, **43**, 198 (2013). Doi: https://doi.org/10.5051/jpis.2013.43.4.198
21. Y. Choi, J. Kim, C. Jeong, Optimization of the Barrier Oxide Layer to Enhance Long-term Corrosion Resistance of SUS 316L Stainless Steel in 3.5 wt% NaCl Solution, *Journal of Materials Science,* **60**, 8148 (2025). Doi: https://doi.org/10.1007/s10853-025-10916-4
22. J. H. Liu, G. L. Wu, M. Yu, L. Wu, Y. Zhang, S. M. Li, Influence of Incremental Rate of Anodising Current on Roughness and Electrochemical Corrosion of Oxide Film on Titanium Alloy Ti–10V–2Fe–3Al, *Surface Engineering,* **28**, 406 (2012). Doi: https://doi.org/10.1179/1743294411Y.0000000091
23. C. Jeong, J. Jung, K. Sheppard, C. H. Choi, Control of the Nanopore Architecture in Anodic Alumina via Stepwise Anodization with Voltage Modulation and pore widening, *Nanomaterials,* **13**, 342 (2023). Doi: https://doi.org/10.3390/nano13020342
24. J. G. Buijnsters, R. Zhong, N. Tsyntsaru, J. P. Celis, Surface Wettability of Macroporous Anodized Aluminum

Oxide, *ACS Applied Materials & Interfaces,* **5**, 3224 (2013). Doi: https://doi.org/10.1021/am4001425

25. W. Zhang, L. Huang, C. Zi, Y. Cai, Y. Zhang, X. Zhou, F. Shang, L. Zhao, Y. Liu, G. Li, Wettability of Porous Anodic Aluminum Oxide Membranes with Three-dimensional, Layered Nanostructures, *Journal of Porous Materials,* **25**, 1707 (2018). Doi: https://doi.org/10.1007/s10934-018-0584-5
26. N. Costa, P. Li, J. Liang, S. Shivkumar, Effect of Contact Angle on the Morphology of Nanostructures Produced by Solution wetting of Anodized Aluminum Oxide Templates, *Journal of Nanoparticle Research*, **20**, 103 (2018). Doi: https://doi.org/10.1007/s11051-018-4204-8
27. J. Ye, Q. Yin, Y. Zhou, Superhydrophilicity of Anodic Aluminum Oxide Films: From "Honeycomb"to "bird's nest", *Thin Solid Films*, **517**, 6012 (2009). Doi: https://doi.org/10.1016/j.tsf.2009.04.042
28. K. M. Kang, S. Choi, Y. C. Nah, Technological Trends in a Local Anodization, *Journal of Surface Science and Engineering*, **56**, 115 (2023). Doi: https://doi.org/10.5695/JSSE.2023.56.2.115
29. T, Hasebe, R. S. Alwitt, Nonlinear Dielectric Properties of Anodic Aluminum Oxide Films, *Journal of The Electrochemical Society*, **154**, C626 (2007). Doi: https://doi.org/10.1149/1.2776219
30. S. G. Lim, H. C. Choe, Bioactive apatite formation on PEO-treated Ti-6Al-4V alloy after 3rd anodic titanium oxidation, *Applied Surface Science*, **484**, 365 (2019). Doi: https://doi.org/10.1016/j.apsusc.2019.04.096
31. H. Masuda, K, Yada and A. Osaka, Self-ordering of Cell Configuration of Anodic Porous Alumina with Large-size Pores in Phosphoric Acid Solution, *Japanese Journal of Applied Physices*, **37**, L1340 (1998). Doi: https://doi.org/10.1143/JJAP.37.L1340
32. C. C. Chen, J. H. Chen and C. G. Chao, Post-treatment Method of Producing Ordered Arrays of Anodic Aluminum Oxide Using General Purity Commercial (99.7%) Aluminum, *Japanese Journal of Applied Physices*, **44**, 1529 (2005). Doi: https://doi.org/10.1143/JJAP.44.1529
33. H. Ji and C. Jeong, Fabrication of Superhydrophobic Aluminum Alloy Surface with Hierarchical Pore Nanostructure for Anti-Corrosion, *Corrosion Science and Technology*, **18**, 228 (2019). Doi: https://doi.org/10.14773/cst.2019.18.6.228
34. L. Zaraska, G. D. Sulka and M. Jaskula, Anodic Alumina Membranes with Defined Pore Diameters and Thicknesses Obtained by Adjusting the Anodizing Duration and Pore Opening/Widening Time, *Journal of Solid State Electrochemistry*, **15**, 2427 (2011). Doi: https://doi.org/10.1007/s10008-011-1471-z
35. S. M. Suchitra, P. R. Reddy, and N. K. Udayashankar, Effect of Pore Widening Time on the Structural Aspects of Self-Organized Nanopore Arrays Formed by Anodization of Aluminum in Chromic Acid, *Materialstoday: Proceedings*, **3**, 2042 (2016). Doi: https://doi.org/10.1016/j.matpr.2016.04.107
36. Y. Alivov, M. Pandikunta, S. Nikishin, Z.Y. Fan, The Anodization Voltage Influence on the Properties of TiO_2 Nanotubes Grown by Electrochemical Oxidation, *Nanotechnology*, **20**, 225602 (2009). Doi: https://doi.org/10.1088/0957-4484/20/22/225602
37. C. Blawert, W. Dietzel, E. Ghali, Anodizing Treatments for Magnesium Alloys and Their Effect on Corrosion Resistance in Various Environments, *Advanced Engineering Materials*, **8**, 511 (2006). Doi: https://doi.org/10.1002/adem.200500257
38. Y. Wu, C. Zhang, Analysis of Anti-condensation Mechanism on Superhydrophobic Anodic Aluminum Oxide Surface, *Applied thermal engineering*, **58**, 664 (2013). Doi: https://doi.org/10.1016/j.applthermaleng.2013.01.048
39. R. N. Wenzel, Resistance of Solid Surfaces to Wetting by Water, *Industrial & Engineering Chemistry*, **28**, 988 (1936). https://doi.org/10.1021/ie50320a024
40. Y. Choi, C. Jeong, Investigating the Influence of Pore-widening Time Control in Electrochemical Anodization for the Formation of Hybrid Titanium Nanostructures with Enhanced Superhydrophobicity for Improved Corrosion Resistance Efficiency, *Electrochimica Acta*, **492**, 144380 (2024) https://doi.org/10.1016/j.electacta.2024.144380
41. T. C. Gomes, D. Kumar, N. Alves, J. Kettle, L. F. Santos, The Effect of Anodization Parameters on the Aluminum Oxide Dielectric Layer of Thin-Film Transistors, *Journal of Visualized Experiments*, **159**, e60798 (2020). Doi: https://doi.org/10.3791/60798
42. D. Deger, K. Ulutas, S. Yakut, AC conductivity and Dielectric Properties of Al_2O_3 Thin Films, *Journal of Ovonic Research*, **8**, 179 (2012). https://chalcogen.ro/179_Deger.pdf
43. William D. Callister Jr, and David G. Rethwisch, Materials science and engineering: an introduction, 10th ed., John wiley & sons (2020). https://ftp.idu.ac.id/wp-content/uploads/ebook/tdg/TEKNOLOGI%20REKAYASA%20MATERIAL%20PERTAHANAN/Materials%20Science%20and%20Engineering%20An%20Introduction%

20by%20William%20D.%20Callister,%20Jr.,%20David%20G.%20Rethwish%20(z-lib.org).pdf
44. Allan R. Hambley, Electrical engineering: principles and applications, 7th ed., Upper Saddle River: Pearson (2017). https://nirmt.com/storage/uploads/E-BOOK_BE-ELECTRICAL/Electrical%20Engineering%20Principles%20and%20Applications.pdf